Drought-induced decoupling between carbon uptake and tree growth impacts forest carbon turnover time

Title

Drought-induced decoupling between carbon uptake and tree growth impacts forest carbon turnover time

Authors

Steven A. Kannenberg[1*], Antoine Cabon[1], Flurin Babst[2,3], Soumaya Belmecheri[3], Nicolas Delpierre[4,5], Rossella Guerrieri[6], Justin T. Maxwell[7], Frederick C. Meinzer[8], David J.P. Moore[2], Christoforos Pappas[9,10,11], Masahito Ueyama[12], Danielle E.M. Ulrich[13], Steven L. Voelker[14], David R. Woodruff[8], William R.L. Anderegg[1]

[1]School of Biological Sciences, University of Utah, Salt Lake City, UT, USA.

[2]School of Natural Resources and the Environment, University of Arizona, Tucson, AZ, USA.

[3]Laboratory of Tree-Ring Research, University of Arizona, Tucson, AZ, USA.

[4]Université Paris-Saclay, CNRS, AgroParisTech, Ecologie Systématique et Evolution, 91405, Orsay, France.

[5]Institut Universitaire de France (IUF)

[6]Department of Agricultural and Food Sciences, University of Bologna, Bologna, Italy

[7]Department of Geography, Indiana University, Bloomington, IN, USA

[8]USDA Forest Service, Pacific Northwest Research Station, Corvallis, OR, USA

[9]Centre d'étude de la forêt, Université du Québec à Montréal, Montreal, QC, Canada

[10]Département Science et Technologie, Téluq, Université du Québec, Montreal, QC, Canada

[11]Department of Civil Engineering, University of Patras, Rio Patras, Greece

[12]Graduate School of Life and Environmental Sciences, Osaka Prefecture University, Sakai, Japan

[13]Department of Ecology, Montana State University, Bozeman, MT, USA

[14]SUNY College of Environmental Science and Forestry, Syracuse, NY, USA

Corresponding author, s.kannenberg@utah.edu, 612-578-9551

Keywords

GPP, legacy effect, resilience, resistance, tree rings

Abstract

The ability of forests to withstand, and recover from, acute drought stress is a critical uncertainty regarding the impacts of climate change on the terrestrial carbon (C) cycle, but it is unclear how drought responses scale from individual trees to whole forests. Here, we assembled a dataset of tree-ring chronologies co-located within the footprint of eddy covariance towers across North America and Europe, with the aim of quantifying the sensitivity of tree radial growth versus gross primary productivity (GPP) during and following drought. We found that drought induced a large decoupling across C cycle processes, whereby GPP was relatively resistant to water stress despite large reductions in tree-ring widths. This decoupling also occurred in the year following drought (i.e., a 'drought legacy effect'), and was similar in magnitude in response to both summer and winter droughts. By modeling whole-forest C turnover time, we show that a radial growth-GPP decoupling has important ramifications for the forest C cycle, especially if the C not used to support radial growth is instead allocated towards pools with short residence times. Our results demonstrate that quantifications of drought impacts that rely solely on C uptake are missing this fundamental pathway through which drought alters the forest C cycle and the resulting feedbacks to the climate system.

58

59 **Introduction**

60 Forests store nearly half of the carbon (C) in terrestrial ecosystems and take up ~25% of
61 all anthropogenic C emissions (Bonan, 2008; Pan et al., 2011). However, the capacity of forests
62 to assimilate and store C is threatened by an increase in the frequency and severity of droughts
63 (Cook et al., 2015; Dai, 2013; McDowell et al., 2020). The drought resistance (ability to maintain
64 function) and resilience (ability to recover function) of these processes in future climates is a
65 major uncertainty in the terrestrial C cycle (Sippel et al., 2018) yet exerts a significant influence
66 on the climate change mitigation potential of forests worldwide (Anderegg et al., 2020).

67 Current efforts to quantify the resistance and resilience of forests to drought stress have
68 largely been undertaken using tree-ring chronologies (Camarero et al., 2018; Lloret et al., 2011;
69 Merlin et al., 2015). These approaches are invaluable towards understanding the climatic,
70 topographic, and biological mechanisms that underpin the responses of tree growth to drought.
71 However, radial tree growth is only one aspect of a complex forest C cycle, and the relationship
72 between growth and whole-ecosystem fluxes of C is indirect. Thus, several studies have
73 quantified the drought resistance and resilience of C uptake using broader-scale metrics of
74 forest C cycling such as gross primary productivity (GPP) derived from flux towers (He et al.,
75 2018; Shen et al., 2016; Yu et al., 2017). Recent evidence suggests that drought may drive a
76 large decoupling between these processes, whereby structural tree growth is much more
77 sensitive to drought than GPP (Delpierre et al., 2016; Kannenberg et al., 2020b, 2019b).

78 While this decoupling is intuitive at the tissue-level given the higher drought sensitivity
79 of turgor-driven cell expansion than photosynthesis (Hsiao, 1973) and the plasticity of plant C

allocation in response to environmental stress (Epron et al., 2012), evidence at the stand- or ecosystem -scale is scarce due to the paucity of co-located measurements of tree growth and GPP (Babst et al., 2021, though see Cabon et al., 2022 and Krejza et al., 2022). Therefore, our knowledge of the degree of coupling between growth and GPP rests entirely on either case studies from a single drought (Kannenberg et al., 2019b), or GPP proxies from models or remote sensing products that may not fully capture both the magnitude of drought impacts or any lagged recovery processes (Anderegg et al., 2015; Kolus et al., 2019; Stocker et al., 2019). Given this lack of evidence, it is unsurprising that most large-scale vegetation models represent allocation to woody tissues as a constant percentage of GPP (Fatichi et al., 2019). Additional uncertainties regarding these processes arise due to the high species-specificity of drought responses, which are underlain by variability in key functional traits. Uncovering the traits that underlie tree drought responses, as well as the coupling between GPP and growth, has the potential to lead us to an improved predictive understanding of how drought impacts the forest carbon cycle.

Divergent drought impacts on tree growth versus GPP have vast implications for our understanding of the terrestrial C cycle. Large shifts in allocation from tree boles to pools with shorter residence times (Doughty et al., 2015, 2014; Kannenberg et al., 2019b) have consequences for the turnover time of forest C, the magnitude of which is a major uncertainty in current vegetation models (Carvalhais et al., 2014; Friend et al., 2014; Pugh et al., 2020). Quantifying the differential sensitivity of drought resistance and resilience across distinct C cycle processes and scales could provide valuable insights regarding whether drought impacts are likely to be most apparent through decreased C uptake and productivity, and/or through a shortened C turnover time.

Here, we seek to directly test the hypothesis that drought decouples tree radial growth from ecosystem C uptake. To do so, we amassed a dataset of 38 tree ring chronologies (spanning 31 common gymnosperm and angiosperm species) collected at 16 different eddy covariance tower sites (277 total site-years) that have experienced a severe drought. These chronologies represented the majority of the species present within these towers' footprints, enabling direct comparisons between the resistance and resilience of tree growth and stand-scale GPP. We then explored the implications of a decoupling between growth and GPP for the forest C cycle using a 'box model' that includes fluxes in and out of the main pools of tree structural C. We ask:

1) Are drought resistance and resilience decoupled across C cycle processes?

2) What traits shape variability in resistance and resilience, and what controls the degree of decoupling of these indices across scales?

3) What are the implications of a decoupling between tree radial growth and GPP for whole-forest C turnover?

Materials and methods

Sites and eddy covariance data

We compiled a dataset of 38 tree-ring chronologies collected near or within the footprint of 16 different eddy covariance towers (Fig. 1, Table S1). These sites, located across North America and Europe, spanned a wide variety of ecosystem types and were largely representative of various temperate and arid woodland biomes (Fig. 1), yet all experienced a

124 severe summer or winter drought within the flux record (see below for drought definition). All
125 sites are included in either the FLUXNET2015 Tier 1 (Pastorello *et al.* 2020,
126 fluxnet.org/data/fluxnet2015-dataset) or AmeriFlux (ameriflux.lbl.gov, downloaded January 6,
127 2021) datasets.

128 For the 10 sites in the AmeriFlux network (representing 30 chronologies), net ecosystem
129 exchange data (NEE) was gapfilled using the 50th percentile Ustar distribution and then
130 partitioned into GPP using the nighttime method (Reichstein et al., 2005) as implemented in the
131 R package *REddyProc* (Wutzler et al., 2018). Data that were gapfilled by site PIs were
132 preferentially used, if available. If the NEE variable was not available, turbulent CO_2 flux (FC) was
133 used instead. The meteorological data used for partitioning were taken from the primary sensor
134 (the _1_1_1 suffix). During some periods, there were not enough incoming shortwave radiation
135 data to properly gapfill NEE. In these cases, incoming photosynthetically active radiation (if
136 available) was converted to shortwave, under the assumption that half of the incoming solar
137 irradiance is photosynthetically active radiation (Britton and Dodd, 1976). Data from US-UMB
138 from AmeriFlux are aggregated into both 30-minute (years 2007 – 2019) and 60-minute (years
139 2000 – 2014) increments. For this site, we used the full 30-minute record for 2007 – 2019 and
140 the 60-minute record for 2000 – 2006. For FLUXNET sites, we used the nighttime partitioned,
141 variable 50th percentile distribution Ustar GPP product (i.e., GPP_NT_VUT_REF), which is the
142 data product most comparable to our AmeriFlux partitioning approach. We confirmed that our
143 partitioning approach was comparable to the FLUXNET2015 data by comparing a subset of 6
144 sites that were included in both datasets (and thus partitioned independently). At these sites,
145 monthly sums of our GPP product closely matched FLUXNET2015 (r^2 = 0.98, slope not
146 significantly different from one).

147 Some gaps remained even after gapfilling due to sensor malfunction, maintenance, or
148 other long-term gaps. Years with large gaps in GPP during the growing season were excluded
149 from analysis, and the site-years that remained all had < 5% of GPP records missing.

150 In order to make GPP (typically aggregated at 30- or 60-minute resolutions) comparable
151 to detrended tree-ring widths (annual resolution, see below for tree-ring detrending methods),
152 we normalized the GPP time series by summing GPP for each site-year and calculating the
153 anomaly for each annual GPP sum (i.e., the percentage deviation from mean GPP at that site). At
154 11 sites, annual GPP increased or decreased over time, which would bias our calculations of
155 drought responses depending on the year in which the drought occurred. For sites that had a
156 statistically significant (via linear regression, $P < 0.05$) increase or decrease in annual GPP over
157 time, we detrended the GPP time series by taking the residuals of the linear model and
158 normalizing them as above. This quantification of normalized and detrended annual GPP was
159 used for all subsequent analysis.

160

161 *Tree ring data*

162 Canopy dominant or co-dominant trees of the common species at each flux site have
163 been previously cored, processed, measured, and crossdated using standard
164 dendrochronological procedures (Speer, 2012; Stokes and Smiley, 1999). Crossdated ring width
165 measurements were detrended using a spline with a 50% frequency cutoff set at two-thirds of
166 the mean sample length (Klesse, 2021), and species-level chronologies (ring width indices, RWI)
167 were built using a bi-weight robust mean-value approach in the R package *dplR* (Bunn, 2008).
168 The distance of each cored tree to the flux tower varied, but all cores were sampled within 1 km

of the tower. At least 5 trees were cored for each species at each site, though the average number of cores per site was 55 ± 8.0 (mean ± standard error). Chronology lengths ranged from 30 to 300 years, and the average chronology length was 112.9 years ± 9.8 (mean ± standard error). The average expressed population signal (EPS, which quantifies the signal-to-noise ratio of the time series) for our chronologies was 0.87 ± 0.01 (mean ± standard error). Our results were robust to removing chronologies with an EPS lower than the commonly-used threshold of 0.85 (Fig. S1). However, given that this threshold is arbitrary (Buras, 2017) and a low EPS may simply be indicative of less synchronous tree growth within a stand (a dynamic worth capturing in our study), we elected to not remove chronologies with low EPS for subsequent analyses. Chronology information and statistics are available in Table S2.

We also compiled species composition estimates for all cored tree species at each site (Table S3). These estimates were obtained from the published literature where possible. If published data were not found, species composition estimates were taken from site webpages or obtained directly from site research teams. We used plot-based basal area measurements where possible, but needed to use biomass or canopy cover estimates at a small subset of sites. Citations and data sources for these estimates are available in Table S3. When multiple tree species were present at a flux tower site, we calculated a community-weighted mean RWI using these data, in order to increase comparability to whole-ecosystem measurements of GPP.

Forest and plant trait data

Site information of location, elevation, mean annual temperature, mean annual precipitation, and IGBP biome were taken from the respective site pages on the AmeriFlux or

191 FLUXNET2015 websites. Functional traits were collected from a variety of different datasets for
192 each of our sampled tree species, including: wood density from the Global Wood Density
193 Database (Chave et al., 2009), specific leaf area and maximum photosynthetic rate from Maire
194 et al. (2015), and hydraulic traits (P50, the water potential at which 50% of xylem conduits are
195 embolized, and the P50 safety margin, which is the difference between P50 and the minimum
196 water potential observed) from the Xylem Functional Traits database (Gleason et al., 2016). Trait
197 data for the analyzed species are available in Table S4.

198 Drought responses in GPP likely reflect the integrated signal of all constituent species in
199 the tower footprint. Therefore, we aggregated plant trait data to the stand scale in a number of
200 ways: the mean trait value of all cored species, the standard deviation of all cored species, and
201 the mean of all cored species weighted by species composition.

202

203 *Climate data*

204 Standardized Precipitation Evaporation Index v2.6 (SPEI) data for all site-years were
205 used to quantify drought severity (Vicente-Serrano et al., 2010). SPEI data were extracted for
206 two relevant time scales in order to capture the differential effects of growing season versus
207 winter droughts: June – August (hereafter, "Summer") and the previous October – March
208 (hereafter, "Winter").

209 We calculated mean site climatic water deficit (CWD) as potential evapotranspiration
210 (PET) minus actual evapotranspiration (AET), using data from the TerraClimate dataset
211 (Abatzoglou et al., 2018). Monthly values CWD were extracted for all sites, and these values
212 were summed to get annual CWD. Mean site CWD was calculated over the period 2000 – 2019

213 in order to reflect climatic conditions during the years when most of our flux tower data were
214 present.

215

216 *MODIS data*

217 MODIS leaf area index (LAI) over 8-days windows (MCD15A2H, 500 m pixel size) were
218 obtained for each site from 2002 – 2019 using the R package *MODISTools* (Tuck et al., 2014). In
219 order to make MODIS data comparable to annual GPP sums in ecosystems that experience large
220 annual variation in LAI (e.g., deciduous forests), we limited LAI data to the growing season in
221 each year using a previously published method (Kannenberg et al., 2020a). We considered the
222 start of the growing season to be the first day at which a smoothed curve of daily GPP sums
223 crossed a threshold of mean winter GPP + 30% of the annual smoothed GPP amplitude, and the
224 end of the growing season to be the last time point when smoothed GPP fell below this
225 threshold. Annual growing season LAI means were used in the calculation of drought indices
226 (detailed below), while growing season LAI was also averaged over the entire time interval (2002
227 – 2019) to calculate mean site LAI and thus quantify the typical canopy cover at each site.

228

229 *Calculation of drought indices*

230 To quantify the responses of RWI, GPP, and LAI to severe drought, we calculated metrics
231 of drought resistance and resilience. First, we identified severe drought years within the eddy
232 covariance record at each site. We defined a severe drought as a < -1.5 anomaly in SPEI during
233 two different periods: summer (June – August, the peak growing season) and winter (the

234 previous October – March, the start of the hydrological year to early spring). These two periods
235 were chosen to capture any differential effects of a hotter, acute growing season drought (i.e.,
236 summer drought) versus a longer-term anomaly in early season moisture storage (i.e., winter
237 drought). Our results were nearly identical when defining a summer drought as the full growing
238 season (April – September), due to significant overlap between the drought years identified with
239 each method (Fig. S2). Any multi-year droughts (i.e., two sequential winter or summer drought
240 years < -1.5 SPEI) were identified and not considered in our analyses to avoid any bias
241 introduced by a few anomalously severe droughts. Likewise, multi-drought years (i.e., a winter
242 and summer drought in the same year) were not included in the analysis (see Table S1 for the
243 drought site-years that were included in our analyses). The selected threshold of drought
244 severity was chosen to represent a severe drought that impacts forest function, yet also be
245 common enough to have a reasonable sample size in our dataset. The threshold of -1.5 SPEI,
246 which corresponds to a return period of 20 years across all sites in our dataset (range = 10 to 33-
247 year return period), is comparable with other studies that have quantified severe drought
248 resistance and resilience (Anderegg et al., 2015; Kannenberg, Maxwell, et al., 2019). Our main
249 results were robust to relaxing our threshold to -1.2 SPEI (roughly a drought every 8 years, Fig.
250 S3). When increasing our threshold to -2 SPEI (a once per century event), our sample size
251 decreased drastically to only 4 drought events across all sites (Fig. S4).

252 Once these severe drought years were identified, we calculated drought resistance (Rt)
253 and resilience (Rs) for the community-weighted RWI (hereafter referred to as "RWI"), annual
254 normalized GPP, and mean growing season LAI as follows:

255 $$Rt = X_{Drought} / \underline{X_{Non-drought}}$$

$$Rs = X_{Drought+1} / \underline{X_{Non-drought}}$$

Where $X_{Drought}$ represents the process of interest (i.e., RWI, GPP, LAI) during the drought year itself, $X_{Drought+1}$ represents the process of interest in the year following a drought, and $\underline{X_{Non-drought}}$ represents the mean of that process in all non-drought years. Thus, these indices are analogous to effect sizes, where Rt represents the impact of each drought on the process of interest relative to normal conditions, and Rs represents the degree to which that process recovered in the year following the drought. These metrics are a slight modification of those developed by Lloret *et al.* (2011), intended to remove noise related to variability in the pre-drought year (Kannenberg et al., 2019b). Finally, the degree of decoupling between GPP and RWI (denoted ΔRt or ΔRs) was calculated as Rt or Rs in GPP minus Rt or Rs in RWI.

C turnover time model

In order to quantify the impact of C reallocation away from stem growth and towards other structural tissues, we modeled the mean turnover time of whole-forest structural C using a simple four-pool vegetation C model under a range of different scenarios, whereby the C not allocated to stem growth during the drought year and following year (i.e., Rt and Rs) was re-allocated entirely to leaf, coarse root, or fine root pools instead. Due to the large uncertainties regarding the residence times and allocation dynamics of reproductive tissues and non-structural pools (e.g., sugars/starches, root exudates, respiratory losses), we elected to constrain our analyses to non-reproductive structural components.

To do so, we compiled data for total biomass C density (aboveground and belowground biomass in Mg C ha^{-1}) for the year 2010 from the 300 m grid cell containing all the flux tower sites using the dataset of Spawn *et al.* (2020). These biomass estimates are almost entirely reflective of tree cover (as opposed to understory vegetation or seedlings) since the underlying dataset for forest biomass is largely based on observations of saplings and mature trees.

After converting to total biomass C within each grid cell (Mg C), that biomass C was partitioned out to each sampled species using our species composition estimates (Table S3). We then allocated that C to leaf, aboveground woody biomass (AWB), coarse root, and fine root pools for each species using allometry derived from the Biomass And Allometry Database (BAAD, Falster *et al.* (2015), Table S5). For our species, all entries in BAAD that had measurements of total plant mass were considered after entries associated with greenhouse and growth chamber studies were excluded to avoid biases associated with the allometry of seedlings and saplings. From these data, mean percent of biomass contained in leaves, AWB (boles and branches), coarse roots, and fine roots were calculated. Many of our species were not present in this dataset, and thus data were aggregated to the family level or to the plant functional type level (i.e., deciduous angiosperm, deciduous conifer, or evergreen conifer). In some cases, our allometric estimates across tissues had a sum greater than one (expected since these tissue-specific estimates are many times drawing on different data sources). In those cases, values were scaled to sum to one. In order to account for tissue-specific differences in C content, we then scaled these estimates by the percentage of C contained in each tissue. Percent C (by dry mass) data for each tissue were obtained for all species from the TRY database (Kattge *et al.* 2020, Table S6), and gaps were filled using family-level and then functional type-level means as above.

299 The effect of drought on AWB was estimated by quantifying the reduction in basal area
300 increment (BAI) in each species during the drought year itself and in the year after (i.e., Rt and
301 Rs). BAI chronologies were constructed using the 'inside-out' approach in the R package *dplR*
302 (Bunn, 2008). We used this method because diameter measurements were not available for
303 many of our sites.

304 Reductions in total aboveground woody C (AWC) were estimated by multiplying total
305 AWC by the reduction in stand basal area (the sum of chronology BAI) C represented by the Rt +
306 Rs tree rings. We then simulated the impacts of a re-allocation of AWC on whole-forest C
307 turnover time by adding that lost AWC entirely to leaf, coarse root, or fine root pools.

308 Whole-forest C turnover time was calculated as follows. First, tissue-specific C density
309 data were converted into a turnover flux (F_{tissue}, in Mg C yr^{-1}) by dividing the total C in each tissue
310 for each species at each site by the mean lifespan (in years) of that tissue (Table S7). Leaf, fine
311 root, and coarse root lifespan data were directly available from TRY, and AWB life span was
312 considered as the mean plant age. Leaf lifespan data for deciduous species were considered to
313 be one year. Tissue lifespan data were aggregated from TRY for each species, and gaps in tissue
314 lifespan data were filled by family and then functional type means. Then, we weighted each
315 tissue-specific F_{tissue} by that species' allometry in order to derive a whole-tree turnover flux, F_{tree}.

316 $$F_{tree} = \sum (F_{tissue} \times Frac_{tissue})$$

317 Where F_{tissue} represents the turnover flux of each structural tissue (leaves, AWB, coarse
318 roots, and fine roots) and $Frac_{tissue}$ represents the proportion of total tree biomass contained in
319 each tissue. F_{tree} was then scaled to the whole forest by weighting the F_{tree} of each species by its
320 fractional of total stand basal area.

$$F_{forest} = \sum (F_{tree} \times Frac_{species})$$

Where $Frac_{species}$ represents the proportion of total species composition for each species at each site. Whole-forest C turnover time, τ (in years), was then calculated as the ratio of whole-forest total C density (C_{forest}) to F_{forest} (Pugh et al., 2020; Sierra et al., 2017).

$$\tau = \frac{C_{forest}}{F_{forest}}$$

Finally, we derived a percent change in τ for each of our tissue allocation scenarios, compared to a scenario where there was no reduction in AWC due to drought (i.e., Rt and Rs were 1). Note that this percentage represents the change in whole-forest τ due entirely to allocation shifts in structural C during the drought year itself and the year after, not changes to τ over longer time scales.

Statistical analysis

Comparisons between categorical variables were conducted using two-tailed t-tests or via pairwise Tukey's HSD for multiple comparisons. Trait correlations were assessed using ordinary least squares regression. For these regressions, normality and homoscedasticity of residuals were confirmed using quantile-quantile and residual plots and were natural log or square root transformed if necessary. All analyses were conducted in the R 4.0 computing environment (R Core Team 2021).

Results

Drought resistance (Rt) and resilience (Rs) in radial tree growth varied widely across species and sites (Fig. S5-S6). Averaged across all drought occurrences, drought reduced community-weighted RWI by 25.4% during the year of the drought itself (i.e., resistance) and by 21.1% in the year after (i.e., resilience, Fig. 2). Lagged drought effects on growth were apparent only one year, with the exception that RWI was significantly reduced for two years following a summer drought (Fig. S7). Rt and Rs were also comparable in response to winter versus summer droughts (Fig. 2). Contrary to the large observed reductions in RWI during and post-drought, annual GPP and growing season LAI remained relatively unchanged, as Rt and Rs were not significantly reduced below one (Fig. 1, Fig. S8-S10).

In general, Rt was correlated with various plant- and site-level traits while Rs was not, though in some cases these relationships differed for summer versus winter droughts (Fig. 3, Fig. S11). Rt calculated from RWI was highest in gymnosperm species and associated with low specific leaf area (SLA) and wood density (WD), though the correlation with WD was not significant following winter droughts. No traits were found to be correlated with Rs calculated from RWI. The traits that predicted Rt and Rs were less consistent for indices derived from GPP. For example, mean P50, mean site precipitation, and mean site water deficit were strong predictors of Rt in response to summer droughts, while there were no significant correlations with Rs. In contrast, Rt in response to winter droughts was best predicted by mean SLA, SLA variability, and P50 variability, while Rs in response to winter droughts was strongly correlated with mean maximum photosynthetic capacity (Amax) and mean LAI.

The degree of decoupling between RWI and GPP Rt during a summer drought was best explained by broad site factors such as elevation ($P < 0.05$, $R^2 = 0.25$) and gymnosperm fraction ($P < 0.05$, $R^2 = 0.20$) instead of plant traits (Fig. 4), though these factors were less successful in

364 explaining the decoupling in Rs. No correlations were found between the degree of RWI-GPP
365 decoupling and any site factors or plant traits following a winter drought.

366 As a way of estimating the C cycle impacts of the observed decoupling between RWI and
367 GPP, we modeled changes to whole-forest C turnover time (τ) under a range of scenarios,
368 whereby the C not allocated to tree-ring widths was instead allocated to other structural pools.
369 We found ubiquitous decreases in τ across all allocation scenarios (Fig. 5, all $P < 0.01$). Declines
370 in τ were particularly pronounced if C was allocated to leaves (mean change in τ = -3.3%), due to
371 the large amount of biomass held in foliage and its short lifespan. Decreases in τ were present,
372 but smaller, if C was allocated belowground (-1.2%), due to the small percentage of total
373 biomass held in fine roots (mean = 4.5% of total biomass) and the longer lifespan of coarse roots
374 (mean = 13.75 yrs).

375

376 **Discussion**

377 *Drought decouples GPP and growth*

378 We found that drought induced a striking decoupling between community-weighted
379 tree growth and stand-scale C dynamics, whereby RWI was significantly reduced in the year of,
380 and the year after, drought, while total annual GPP and mean LAI were unchanged. While RWI,
381 GPP, and LAI have been known to covary in some cases (Campioli et al., 2016; Teets et al., 2017;
382 Xu et al., 2017), our results add to growing evidence that radial growth and canopy-scale C
383 processes are commonly decoupled (Cabon et al., 2022; Delpierre et al., 2016; Mund et al.,
384 2010; Pappas et al., 2020; Rocha et al., 2006; Seftigen et al., 2018).

We also found the magnitude of Rt and Rs in radial growth to be comparable in response to both summer and winter droughts. Given the strong temperature seasonality at most of our sites, the impacts of winter droughts are likely manifest through reductions in spring water balance and/or an increase in freeze-thaw induced root embolism due to decreased soil insulation from snowpack (Love et al., 2019; Venturas et al., 2017). While many studies on drought responses focus on droughts that occur in the growing season, our results point to the large potential for winter droughts to alter forest C cycling in both arid and mesic forests.

Correlations between drought indices and plant- or site-level traits were generally sparse, though we did find a significant linkage between Rt in radial growth and factors pertaining to investment in tissue longevity such as SLA and WD. Consequently, gymnosperm species had the highest Rt in RWI. There is a robust literature documenting the relationship between investment into leaf longevity and tolerance to environmental stressors, including drought (Wright et al., 2004). Thinner leaves (and leaves in angiosperms generally) are less of a C investment for a tree, and are indicative of a life history strategy more tuned towards fast growth in favorable environmental conditions, whereas higher leaf C investment (as in most gymnosperms) is indicative of more long-lived, stress tolerant species (Greenwood et al., 2017; Grime, 1979). However, contrary to previous work (Anderegg et al., 2015; Vitasse et al., 2019) we found that Rs was not lower for gymnosperm species. High latitude coniferous forests feature more prominently in our dataset than previous studies, and thus this result may indicate a greater ability of gymnosperms in northern or mesic forests to recover from drought stress. The factors underlying the high Rt in GPP were less clear, though we did confirm previous evidence that found embolism resistance (P50), site aridity, and drought severity to mediate the

407 responses of whole-forest C fluxes to drought (Anderegg et al., 2015; Schwalm et al., 2017; Wu
408 et al., 2018), with lower Rt observed in drier forests and in those with lower mean P50.

409 There is a growing interest in incorporating key plant functional traits to improve the
410 predictive capacity of terrestrial biosphere models (Fatichi et al., 2019; Fisher et al., 2018;
411 Kennedy et al., 2019). However, it stands to reason that different mechanisms control different
412 C cycle processes, and our results confirm that the functional traits underlying drought
413 responses in growth versus C uptake likely differ. Recognizing this nuance is an important factor
414 to consider towards trait-based vegetation modeling.

415 Multiple mechanisms for the decoupling between RWI and GPP have been proposed
416 (reviewed in Kannenberg *et al.* 2020b). A buffering of GPP during drought due to understory
417 species is one such mechanism, though emerging evidence indicates that these species are
418 frequently equally or more drought sensitive than canopy dominant species (Kannenberg et al.,
419 2019b; Rollinson et al., 2021). An abundance of research indicates that a major factor driving
420 this decoupling is likely the weakening of the link between C source activity and radial growth
421 sink dynamics due to: 1) the greater sensitivity of xylogenesis than photosynthesis to aridity, and
422 2) dynamic C allocation processes (Kannenberg et al., 2019b; Körner, 2015; Mund et al., 2010;
423 Pappas et al., 2020; Peters et al., 2021; Rocha et al., 2006). For example, radial growth is often
424 more sensitive to drought than GPP (Delpierre et al., 2016; Martin-StPaul et al., 2017; Peters et
425 al., 2021), and thus the different sensitivities of these processes could result in radial growth
426 reductions without concomitant declines in GPP. Radial growth is likely also actively reduced
427 during and following drought, whereby C is allocated elsewhere such as non-structural carbon
428 (Körner, 2015), root structural and exudate pools (Phillips et al., 2016), or reproductive efforts
429 (Hacket-Pain et al., 2018).

Allocation shifts impact turnover time

No matter if the decoupling between RWI and GPP was due to passive or active mechanisms, the C that was fixed yet not used for radial growth necessarily went towards some other structural or non-structural pools. Allocation of C away from long-lived aboveground woody biomass pools could impart profound changes on the forest C cycle irrespective of any drought-induced decline in GPP, because that C is very likely to be allocated towards tissues or compounds with shorter turnover times (Pappas et al., 2020). We estimated that no matter what structural pool C was allocated to, whole-forest C turnover time (τ) was significantly reduced, and this decline was notably large in the foliar allocation scenario. Given that our drought threshold of -1.5 SPEI represented a roughly 20-year drought frequency, our upper-bound estimate of mean τ (where C was allocated to foliar tissue following a summer drought) implies a 0.39% reduction in τ over the lifespan of the forest assuming steady-state vegetation dynamics. The magnitude of this estimate is striking as it is roughly a sixth of the current trend in forest τ (-2.3%) due to increasing tree mortality (Yu et al., 2019). While significant foliar allocation shifts due to drought have been observed at some of our sites (Kannenberg et al., 2019b), widespread canopy allocation across sites seems unlikely given that we did not observe a significant decrease in Rt or Rs derived from MODIS LAI.

These changes in τ are likely a conservative estimate since we only modeled non-reproductive structural C components, which have relatively long residence times. If C were allocated to respiratory fluxes or non-structural compounds, which generally can turn over within days or weeks (Carbone et al., 2007; Muhr et al., 2016), declines in τ would be even more sizeable. Likewise, large-scale allocation to reproductive efforts (e.g., masting events) frequently occurs during or following drought (Hacket-Pain et al., 2018), and is a plausible mechanism for

453 the decoupling between RWI and GPP that would likely reduce τ. Though, the magnitude of this
454 reduction in turnover τ would be highly species-dependent given the high variability in
455 reproductive allocation and tissue residence time across species (Wenk and Falster, 2015). We
456 also note that our model did not include any decomposition dynamics due to uncertainties in
457 decomposition rate over time and across species. Despite these uncertainties, our results
458 provide a first-order approximation of the impacts of drought-induced allocation shifts on the
459 forest C cycle across a range of scenarios. Crucially, our τ modeling reveals that the degree to
460 which the decoupling between RWI and GPP impacts the forest C cycle hinges on where that C is
461 allocated. Further efforts in model development, coupled with increased measurement of
462 allometry and C allocation during and after drought, are necessary steps towards refining our
463 estimates of how this decoupling will impact the ability of forests to mitigate climate change.

464 *Conclusions*

465 Drought is likely to cause consequential impacts to the terrestrial C cycle through
466 changes in C uptake, forest structure, and mortality rates (Saatchi et al., 2013; Yang et al., 2018;
467 Yu et al., 2019). Here, we document widespread and direct evidence of an additional, and
468 underappreciated, impact of drought on the forest C cycle: a fundamental disconnect between
469 the responses of tree radial growth versus whole-forest C uptake. We estimate that a drought-
470 induced allocation of C away from radial growth leads to decreases in whole-forest C turnover
471 time. This evidence indicates that drought impacts on terrestrial C cycling may be significantly
472 mediated by C allocation processes, irrespective of C uptake. Crucially, satellite-based estimates
473 of drought impacts or vegetation models driven by photosynthetic or productivity dynamics may
474 be missing key pathways through which the C cycle will be altered in a changing climate with
475 more frequent and severe drought.

Acknowledgements

We thank Ross Alexander and Chad Hanson for contributing tree-ring data, and Seth Spawn for assistance extracting biomass carbon density data. Funding for AmeriFlux data resources were provided by the DOE Office of Science. SAK is supported by the NSF Ecosystem Science cluster grant #1753845, the USDA Forest Service Forest Health Protection Evaluation Monitoring program grant #19-05, and the DOE Environmental System Science program grant #DE-SC0022052. MU is supported by the Arctic Challenge for Sustainability II (JPMXD1420318865). JTM acknowledges support from the US Department of Agriculture National Institute of Food and Agriculture, Agricultural and Food Research Initiative Competitive Program #2017-67013-26191 and Indiana University Vice Provost of Research Faculty.

References

Abatzoglou, J.T., Dobrowski, S.Z., Parks, S.A., Hegewisch, K.C., 2018. TerraClimate, a high-resolution global dataset of monthly climate and climatic water balance from 1958-2015. Sci. Data 5, 1–12. https://doi.org/10.1038/sdata.2017.191

Anderegg, W.R.L., Schwalm, C., Biondi, F., Camarero, J.J., Koch, G., Litvak, M., Ogle, K., Shaw, D., Shevliakova, E., Williams, A.P., Wolf, A., Ziaco, E., Pacala, S., 2015. Pervasive drought legacies in forest ecosystems and their implications for carbon cycle models. Science (80-.). 349, 528–532. https://doi.org/10.1017/CBO9781107415324.004

Anderegg, W.R.L., Trugman, A.T., Badgley, G., Anderson, C.M., Bartuska, A., Ciais, P., Cullenward, D., Field, C.B., Freeman, J., Goetz, S.J., Hicke, J.A., Huntzinger, D., Jackson, R.B., Nickerson,

498 J., Pacala, S., Randerson, J.T., 2020. Climate-driven risks to the climate mitigation potential
499 of forests. Science (80-.). 368. https://doi.org/10.1126/science.aaz7005

500 Babst, F., Friend, A.D., Karamihalaki, M., Wei, J., von Arx, G., Papale, D., Peters, R.L., 2021.
501 Modeling Ambitions Outpace Observations of Forest Carbon Allocation. Trends Plant Sci.
502 26, 210–219. https://doi.org/10.1016/j.tplants.2020.10.002

503 Bonan, G.B., 2008. Forests and climate change: Forcings, feedbacks, and the climate benefits of
504 forests. Science (80-.). 320, 1444–1449.

505 Britton, C., Dodd, J., 1976. Relationships of photosynthetically active radiation and shortwave
506 irradiance. Agric. Meteorol. 17, 1–7.

507 Bunn, A.G., 2008. A dendrochronology program library in R (dplR). Dendrochronologia 26, 115–
508 124. https://doi.org/10.1016/j.dendro.2008.01.002

509 Buras, A., 2017. A comment on the expressed population signal. Dendrochronologia 44, 130–
510 132. https://doi.org/10.1016/j.dendro.2017.03.005

511 Camarero, J.J., Gazol, A., Sangüesa-Barreda, G., Cantero, A., Sánchez-Salguero, R., Sánchez-
512 Miranda, A., Granda, E., Serra-Maluquer, X., Ibáñez, R., 2018. Forest Growth Responses to
513 Drought at Short- and Long-Term Scales in Spain: Squeezing the Stress Memory from Tree
514 Rings. Front. Ecol. Evol. 6. https://doi.org/10.3389/fevo.2018.00009

515 Campioli, M., Malhi, Y., Vicca, S., Luyssaert, S., Papale, D., Peñuelas, J., Reichstein, M.,
516 Migliavacca, M., Arain, M.A., Janssens, I.A., 2016. Evaluating the convergence between
517 eddy-covariance and biometric methods for assessing carbon budgets of forests. Nat.
518 Commun. 7, 13717. https://doi.org/10.1038/ncomms13717

519 Carbone, M.S., Czimczik, C.I., McDuffee, K.E., Trumbore, S.E., 2007. Allocation and residence
520 time of photosynthetic products in a boreal forest using a low-level 14C pulse-chase
521 labeling technique. Glob. Chang. Biol. 13, 466–477. https://doi.org/10.1111/j.1365-
522 2486.2006.01300.x

523 Carvalhais, N., Forkel, M., Khomik, M., Bellarby, J., Jung, M., Migliavacca, M., Mu, M., Saatchi, S.,
524 Santoro, M., Thurner, M., Weber, U., Ahrens, B., Beer, C., Cescatti, A., Randerson, J.T.,
525 Reichstein, M., 2014. Global covariation of carbon turnover times with climate in terrestrial
526 ecosystems. Nature 514, 213–217. https://doi.org/10.1038/nature13731

527 Chave, J., Coomes, D., Jansen, S., Lewis, S.L., Swenson, N.G., Zanne, A.E., 2009. Towards a
528 worldwide wood economics spectrum. Ecol. Lett. 12, 351–366.
529 https://doi.org/10.1111/j.1461-0248.2009.01285.x

530 Cook, B.I., Ault, T.R., Smerdon, J.E., 2015. Unprecedented 21st century drought risk in the
531 American Southwest and Central Plains. Sci. Adv. 1.
532 https://doi.org/10.1126/sciadv.1400082

533 Dai, A., 2013. Increasing drought under global warming in observations and models. Nat. Clim.
534 Chang. 3, 52–58. https://doi.org/10.1038/nclimate1633

535 Delpierre, N., Berveiller, D., Granda, E., Dufrêne, E., 2016. Wood phenology, not carbon input,
536 controls the interannual variability of wood growth in a temperate oak forest. New Phytol.
537 210, 459–470. https://doi.org/10.1111/nph.13771

538 Doughty, C.E., Malhi, Y., Araujo-Murakami, A., Metcalfe, D.B., Silva-Espejo, J., Arroyo, L.,
539 Heredia, J.P., Pardo-Toledo, E., Mendizabal, L.M., Rojas-Landivar, V., Vega-Martinez, M.,

Flores-Valencia, M., Sibler-Rivero, R., Moreno-Vare, L., Viscarra, L., Chuviru-Castro, T., M, O.-B., Ledezma, R., 2014. Allocation trade-offs dominate the response of tropical forest growth to seasonal and interannual drought. Ecology 95, 2192–2201. https://doi.org/10.1890/13-1507.1

Doughty, C.E., Metcalfe, D.B., Girardin, C. a. J., Amézquita, F.F., Cabrera, D.G., Huasco, W.H., Silva-Espejo, J.E., Araujo-Murakami, a., da Costa, M.C., Rocha, W., Feldpausch, T.R., Mendoza, a. L.M., da Costa, a. C.L., Meir, P., Phillips, O.L., Malhi, Y., 2015. Drought impact on forest carbon dynamics and fluxes in Amazonia. Nature 519, 78–82. https://doi.org/10.1038/nature14213

Epron, D., Bahn, M., Derrien, D., Lattanzi, F.A., Pumpanen, J., Gessler, A., Högberg, P., Maillard, P., Dannoura, M., Gérant, D., Buchmann, N., 2012. Pulse-labelling trees to study carbon allocation dynamics: a review of methods, current knowledge and future prospects. Tree Physiol. 32, 776–98. https://doi.org/10.1093/treephys/tps057

Falster, D.S., Duursma, R.A., Ishihara, M.I., Barneche, D.R., FitzJohn, R.G., Vårhammar, A., Aiba, M., Ando, M., Anten, N., Aspinwall, M.J., Baltzer, J.L., Baraloto, C., Battaglia, M., Battles, J.J., Lamberty, B.B., Van Breugel, M., Camac, J., Claveau, Y., Coll, L., Dannoura, M., Delagrange, S., Domec, J.C., Fatemi, F., Feng, W., Gargaglione, V., Goto, Y., Hagihara, A., Hall, J.S., Hamilton, S., Harja, D., Hiura, T., Holdaway, R., Hutley, L.B., Ichie, T., Jokela, E.J., Kantola, A., Kelly, J.W.G., Kenzo, T., King, D., Kloeppel, B.D., Kohyama, T., Komiyama, A., Laclau, J.P., Lusk, C.H., Maguire, D.A., Le Maire, G., Mäkelä, A., Markesteijn, L., Marshall, J., McCulloh, K., Miyata, I., Mokany, K., Mori, S., Myster, R.W., Nagano, M., Naidu, S.L., Nouvellon, Y., O'Grady, A.P., O'Hara, K.L., Ohtsuka, T., Osada, N., Osunkoya, O.O., Peri, P.L.,

562 Petritan, A.M., Poorter, L., Portsmuth, A., Potvin, C., Ransijn, J., Reid, D., Ribeiro, S.C.,
563 Roberts, S.D., Rodríguez, R., Acosta, A.S., Santa-Regina, I., Sasa, K., Selaya, N.G., Sillett, S.C.,
564 Sterck, F., Takagi, K., Tange, T., Tanouchi, H., Tissue, D., Umehara, T., Utsugi, H.,
565 Vadeboncoeur, M.A., Valladares, F., Vanninen, P., Wang, J.R., Wenk, E., Williams, R., De
566 Aquino Ximenes, F., Yamaba, A., Yamada, T., Yamakura, T., Yanai, R.D., York, R.A., 2015.
567 BAAD: A Biomass And Allometry Database for woody plants. Ecology 96, 1445.
568 https://doi.org/10.1890/14-1889.1

569 Fatichi, S., Pappas, C., Zscheischler, J., Leuzinger, S., 2019. Modelling carbon sources and sinks in
570 terrestrial vegetation. New Phytol. 221, 652–668. https://doi.org/10.1111/nph.15451

571 Fisher, R.A., Christoffersen, O., Longo, M., Viskari, T., Koven, C.D., Anderegg, W.R.L., Dietze,
572 M.C., Farrior, C.E., Holm, J.A., Hurtt, G.C., Knox, R.G., Muller-landau, H.C., Lawrence, P.J.,
573 Lichstein, J.W., Shuman, J.K., Verbeeck, H., Powell, T.L., Serbin, S.P., Smith, B., Xu, C.,
574 Moorcroft, P.R., 2018. Vegetation demographics in Earth System Models : A review of
575 progress and priorities. Glob. Chang. Biol. 24, 35–54. https://doi.org/10.1111/gcb.13910

576 Friend, A.D., Lucht, W., Rademacher, T.T., Keribin, R., Betts, R., Cadule, P., Ciais, P., Clark, D.B.,
577 Dankers, R., Falloon, P.D., Ito, A., Kahana, R., Kleidon, A., Lomas, M.R., Nishina, K., Ostberg,
578 S., Pavlick, R., Peylin, P., Schaphoff, S., Vuichard, N., Warszawski, L., Wiltshire, A.,
579 Woodward, F.I., 2014. Carbon residence time dominates uncertainty in terrestrial
580 vegetation responses to future climate and atmospheric CO2. Proc. Natl. Acad. Sci. U. S. A.
581 111, 3280–3285. https://doi.org/10.1073/pnas.1222477110

582 Gleason, S.M., Westoby, M., Jansen, S., Choat, B., Hacke, U.G., Pratt, R.B., Bhaskar, R., Brodribb,
583 T.J., Bucci, S.J., Cao, K., Fan, Z., Feild, T.S., Jacobsen, A.L., Johnson, D.M., Domec, J.,

584 Mitchell, P.J., Morris, H., Nardini, A., Pittermann, J., Schreiber, S.G., Sperry, J.S., Wright, I.J.,
585 Zanne, A.E., 2016. Weak tradeoff between xylem safety and xylem-specific hydraulic
586 efficiency across the worlds woody plant species. New Phytol. 209, 123–136.

587 Greenwood, S., Ruiz-Benito, P., Martínez-Vilalta, J., Lloret, F., Kitzberger, T., Allen, C.D.,
588 Fensham, R., Laughlin, D.C., Kattge, J., Bönisch, G., Kraft, N.J.B., Jump, A.S., 2017. Tree
589 mortality across biomes is promoted by drought intensity, lower wood density and higher
590 specific leaf area. Ecol. Lett. 20, 539–553. https://doi.org/10.1111/ele.12748

591 Grime, J., 1979. Plant strategies and vegetation processes. John Wiley & Sons, Ltd., New York,
592 NY.

593 Hacket-Pain, A.J., Ascoli, D., Vacchiano, G., Biondi, F., Cavin, L., Conedera, M., Drobyshev, I.,
594 Liñán, I.D., Friend, A.D., Grabner, M., Hartl, C., Kreyling, J., Lebourgeois, F., Levanič, T.,
595 Menzel, A., van der Maaten, E., van der Maaten-Theunissen, M., Muffler, L., Motta, R.,
596 Roibu, C.C., Popa, I., Scharnweber, T., Weigel, R., Wilmking, M., Zang, C.S., 2018.
597 Climatically controlled reproduction drives interannual growth variability in a temperate
598 tree species. Ecol. Lett. 21, 1833–1844. https://doi.org/10.1111/ele.13158

599 He, B., Liu, J., Guo, L., Wu, X., Xie, X., Zhang, Y., Chen, C., Zhong, Z., Chen, Z., 2018. Recovery of
600 Ecosystem Carbon and Energy Fluxes From the 2003 Drought in Europe and the 2012
601 Drought in the United States. Geophys. Res. Lett. 45, 4879–4888.
602 https://doi.org/10.1029/2018GL077518

603 Hsiao, T.C., 1973. Plant responses to water stress. Annu. Rev. Plant Physiol. 24, 519–570.

604 Kannenberg, S.A., Bowling, D.R., Anderegg, W.R.L., 2020a. Hot moments in ecosystem fluxes:

High GPP anomalies exert outsized influence on the carbon cycle and are differentially driven by moisture availability across biomes. Environ. Res. Lett. 15. https://doi.org/10.1088/1748-9326/ab7b97

Kannenberg, S.A., Maxwell, J.T., Pederson, N., D'Orangeville, L., Ficklin, D.L., Phillips, R.P., 2019a. Drought legacies are dependent on water table depth, wood anatomy and drought timing across the eastern US. Ecol. Lett. 22, 119–127. https://doi.org/10.1111/ele.13173

Kannenberg, S.A., Novick, K.A., Alexander, M.R., Maxwell, J.T., Moore, D.J.P., Phillips, R.P., Anderegg, W.R.L., 2019b. Linking drought legacy effects across scales: From leaves to tree rings to ecosystems. Glob. Chang. Biol. 25, 2978–2992. https://doi.org/10.1111/gcb.14710

Kannenberg, S.A., Schwalm, C.R., Anderegg, W.R.L., 2020b. Ghosts of the past: how drought legacy effects shape forest functioning and carbon cycling. Ecol. Lett. 23, 891–901. https://doi.org/10.1111/ele.13485

Kattge, J., Bönisch, G., Díaz, S., Lavorel, S., Prentice, I.C., Leadley, P., Tautenhahn, S., Werner, G.D.A., Aakala, T., Abedi, M., Acosta, A.T.R., Adamidis, G.C., Adamson, K., Aiba, M., Albert, C.H., Alcántara, J.M., Alcázar C, C., Aleixo, I., Ali, H., Amiaud, B., Ammer, C., Amoroso, M.M., Anand, M., Anderson, C., Anten, N., Antos, J., Apgaua, D.M.G., Ashman, T.L., Asmara, D.H., Asner, G.P., Aspinwall, M., Atkin, O., Aubin, I., Baastrup-Spohr, L., Bahalkeh, K., Bahn, M., Baker, T., Baker, W.J., Bakker, J.P., Baldocchi, D., Baltzer, J., Banerjee, A., Baranger, A., Barlow, J., Barneche, D.R., Baruch, Z., Bastianelli, D., Battles, J., Bauerle, W., Bauters, M., Bazzato, E., Beckmann, M., Beeckman, H., Beierkuhnlein, C., Bekker, R., Belfry, G., Belluau, M., Beloiu, M., Benavides, R., Benomar, L., Berdugo-Lattke, M.L., Berenguer, E., Bergamin, R., Bergmann, J., Bergmann Carlucci, M., Berner, L., Bernhardt-Römermann, M., Bigler, C.,

627 Bjorkman, A.D., Blackman, C., Blanco, C., Blonder, B., Blumenthal, D., Bocanegra-González,
628 K.T., Boeckx, P., Bohlman, S., Böhning-Gaese, K., Boisvert-Marsh, L., Bond, W., Bond-
629 Lamberty, B., Boom, A., Boonman, C.C.F., Bordin, K., Boughton, E.H., Boukili, V., Bowman,
630 D.M.J.S., Bravo, S., Brendel, M.R., Broadley, M.R., Brown, K.A., Bruelheide, H., Brumnich, F.,
631 Bruun, H.H., Bruy, D., Buchanan, S.W., Bucher, S.F., Buchmann, N., Buitenwerf, R., Bunker,
632 D.E., Bürger, J., Burrascano, S., Burslem, D.F.R.P., Butterfield, B.J., Byun, C., Marques, M.,
633 Scalon, M.C., Caccianiga, M., Cadotte, M., Cailleret, M., Camac, J., Camarero, J.J., Campany,
634 C., Campetella, G., Campos, J.A., Cano-Arboleda, L., Canullo, R., Carbognani, M., Carvalho,
635 F., Casanoves, F., Castagneyrol, B., Catford, J.A., Cavender-Bares, J., Cerabolini, B.E.L.,
636 Cervellini, M., Chacón-Madrigal, E., Chapin, K., Chapin, F.S., Chelli, S., Chen, S.C., Chen, A.,
637 Cherubini, P., Chianucci, F., Choat, B., Chung, K.S., Chytrý, M., Ciccarelli, D., Coll, L., Collins,
638 C.G., Conti, L., Coomes, D., Cornelissen, J.H.C., Cornwell, W.K., Corona, P., Coyea, M.,
639 Craine, J., Craven, D., Cromsigt, J.P.G.M., Csecserits, A., Cufar, K., Cuntz, M., da Silva, A.C.,
640 Dahlin, K.M., Dainese, M., Dalke, I., Dalle Fratte, M., Dang-Le, A.T., Danihelka, J., Dannoura,
641 M., Dawson, S., de Beer, A.J., De Frutos, A., De Long, J.R., Dechant, B., Delagrange, S.,
642 Delpierre, N., Derroire, G., Dias, A.S., Diaz-Toribio, M.H., Dimitrakopoulos, P.G.,
643 Dobrowolski, M., Doktor, D., Dřevojan, P., Dong, N., Dransfield, J., Dressler, S., Duarte, L.,
644 Ducouret, E., Dullinger, S., Durka, W., Duursma, R., Dymova, O., E-Vojtkó, A., Eckstein, R.L.,
645 Ejtehadi, H., Elser, J., Emilio, T., Engemann, K., Erfanian, M.B., Erfmeier, A., Esquivel-
646 Muelbert, A., Esser, G., Estiarte, M., Domingues, T.F., Fagan, W.F., Fagúndez, J., Falster,
647 D.S., Fan, Y., Fang, J., Farris, E., Fazlioglu, F., Feng, Y., Fernandez-Mendez, F., Ferrara, C.,
648 Ferreira, J., Fidelis, A., Finegan, B., Firn, J., Flowers, T.J., Flynn, D.F.B., Fontana, V., Forey, E.,
649 Forgiarini, C., François, L., Frangipani, M., Frank, D., Frenette-Dussault, C., Freschet, G.T.,

Fry, E.L., Fyllas, N.M., Mazzochini, G.G., Gachet, S., Gallagher, R., Ganade, G., Ganga, F., García-Palacios, P., Gargaglione, V., Garnier, E., Garrido, J.L., de Gasper, A.L., Gea-Izquierdo, G., Gibson, D., Gillison, A.N., Giroldo, A., Glasenhardt, M.C., Gleason, S., Gliesch, M., Goldberg, E., Göldel, B., Gonzalez-Akre, E., Gonzalez-Andujar, J.L., González-Melo, A., González-Robles, A., Graae, B.J., Granda, E., Graves, S., Green, W.A., Gregor, T., Gross, N., Guerin, G.R., Günther, A., Gutiérrez, A.G., Haddock, L., Haines, A., Hall, J., Hambuckers, A., Han, W., Harrison, S.P., Hattingh, W., Hawes, J.E., He, T., He, P., Heberling, J.M., Helm, A., Hempel, S., Hentschel, J., Hérault, B., Hereş, A.M., Herz, K., Heuertz, M., Hickler, T., Hietz, P., Higuchi, P., Hipp, A.L., Hirons, A., Hock, M., Hogan, J.A., Holl, K., Honnay, O., Hornstein, D., Hou, E., Hough-Snee, N., Hovstad, K.A., Ichie, T., Igić, B., Illa, E., Isaac, M., Ishihara, M., Ivanov, L., Ivanova, L., Iversen, C.M., Izquierdo, J., Jackson, R.B., Jackson, B., Jactel, H., Jagodzinski, A.M., Jandt, U., Jansen, S., Jenkins, T., Jentsch, A., Jespersen, J.R.P., Jiang, G.F., Johansen, J.L., Johnson, D., Jokela, E.J., Joly, C.A., Jordan, G.J., Joseph, G.S., Junaedi, D., Junker, R.R., Justes, E., Kabzems, R., Kane, J., Kaplan, Z., Kattenborn, T., Kavelenova, L., Kearsley, E., Kempel, A., Kenzo, T., Kerkhoff, A., Khalil, M.I., Kinlock, N.L., Kissling, W.D., Kitajima, K., Kitzberger, T., Kjøller, R., Klein, T., Kleyer, M., Klimešová, J., Klipel, J., Kloeppel, B., Klotz, S., Knops, J.M.H., Kohyama, T., Koike, F., Kollmann, J., Komac, B., Komatsu, K., König, C., Kraft, N.J.B., Kramer, K., Kreft, H., Kühn, I., Kumarathunge, D., Kuppler, J., Kurokawa, H., Kurosawa, Y., Kuyah, S., Laclau, J.P., Lafleur, B., Lallai, E., Lamb, E., Lamprecht, A., Larkin, D.J., Laughlin, D., Le Bagousse-Pinguet, Y., le Maire, G., le Roux, P.C., le Roux, E., Lee, T., Lens, F., Lewis, S.L., Lhotsky, B., Li, Y., Li, X., Lichstein, J.W., Liebergesell, M., Lim, J.Y., Lin, Y.S., Linares, J.C., Liu, C., Liu, D., Liu, U., Livingstone, S., Llusià, J., Lohbeck, M., López-García, Á., Lopez-Gonzalez, G., Lososová, Z., Louault, F., Lukács, B.A., Lukeš, P.,

673 Luo, Y., Lussu, M., Ma, S., Maciel Rabelo Pereira, C., Mack, M., Maire, V., Mäkelä, A.,
674 Mäkinen, H., Malhado, A.C.M., Mallik, A., Manning, P., Manzoni, S., Marchetti, Z.,
675 Marchino, L., Marcilio-Silva, V., Marcon, E., Marignani, M., Markesteijn, L., Martin, A.,
676 Martínez-Garza, C., Martínez-Vilalta, J., Mašková, T., Mason, K., Mason, N., Massad, T.J.,
677 Masse, J., Mayrose, I., McCarthy, J., McCormack, M.L., McCulloh, K., McFadden, I.R.,
678 McGill, B.J., McPartland, M.Y., Medeiros, J.S., Medlyn, B., Meerts, P., Mehrabi, Z., Meir, P.,
679 Melo, F.P.L., Mencuccini, M., Meredieu, C., Messier, J., Mészáros, I., Metsaranta, J.,
680 Michaletz, S.T., Michelaki, C., Migalina, S., Milla, R., Miller, J.E.D., Minden, V., Ming, R.,
681 Mokany, K., Moles, A.T., Molnár, A., Molofsky, J., Molz, M., Montgomery, R.A., Monty, A.,
682 Moravcová, L., Moreno-Martínez, A., Moretti, M., Mori, A.S., Mori, S., Morris, D., Morrison,
683 J., Mucina, L., Mueller, S., Muir, C.D., Müller, S.C., Munoz, F., Myers-Smith, I.H., Myster,
684 R.W., Nagano, M., Naidu, S., Narayanan, A., Natesan, B., Negoita, L., Nelson, A.S.,
685 Neuschulz, E.L., Ni, J., Niedrist, G., Nieto, J., Niinemets, Ü., Nolan, R., Nottebrock, H.,
686 Nouvellon, Y., Novakovskiy, A., Nystuen, K.O., O'Grady, A., O'Hara, K., O'Reilly-Nugent, A.,
687 Oakley, S., Oberhuber, W., Ohtsuka, T., Oliveira, R., Öllerer, K., Olson, M.E., Onipchenko, V.,
688 Onoda, Y., Onstein, R.E., Ordonez, J.C., Osada, N., Ostonen, I., Ottaviani, G., Otto, S.,
689 Overbeck, G.E., Ozinga, W.A., Pahl, A.T., Paine, C.E.T., Pakeman, R.J., Papageorgiou, A.C.,
690 Parfionova, E., Pärtel, M., Patacca, M., Paula, S., Paule, J., Pauli, H., Pausas, J.G., Peco, B.,
691 Penuelas, J., Perea, A., Peri, P.L., Petisco-Souza, A.C., Petraglia, A., Petritan, A.M., Phillips,
692 O.L., Pierce, S., Pillar, V.D., Pisek, J., Pomogaybin, A., Poorter, H., Portsmuth, A., Poschlod,
693 P., Potvin, C., Pounds, D., Powell, A.S., Power, S.A., Prinzing, A., Puglielli, G., Pyšek, P.,
694 Raevel, V., Rammig, A., Ransijn, J., Ray, C.A., Reich, P.B., Reichstein, M., Reid, D.E.B., Réjou-
695 Méchain, M., de Dios, V.R., Ribeiro, S., Richardson, S., Riibak, K., Rillig, M.C., Riviera, F.,

696 Robert, E.M.R., Roberts, S., Robroek, B., Roddy, A., Rodrigues, A.V., Rogers, A., Rollinson,
697 E., Rolo, V., Römermann, C., Ronzhina, D., Roscher, C., Rosell, J.A., Rosenfield, M.F., Rossi,
698 C., Roy, D.B., Royer-Tardif, S., Rüger, N., Ruiz-Peinado, R., Rumpf, S.B., Rusch, G.M., Ryo,
699 M., Sack, L., Saldaña, A., Salgado-Negret, B., Salguero-Gomez, R., Santa-Regina, I.,
700 Santacruz-García, A.C., Santos, J., Sardans, J., Schamp, B., Scherer-Lorenzen, M.,
701 Schleuning, M., Schmid, B., Schmidt, M., Schmitt, S., Schneider, J. V., Schowanek, S.D.,
702 Schrader, J., Schrodt, F., Schuldt, B., Schurr, F., Selaya Garvizu, G., Semchenko, M.,
703 Seymour, C., Sfair, J.C., Sharpe, J.M., Sheppard, C.S., Sheremetiev, S., Shiodera, S., Shipley,
704 B., Shovon, T.A., Siebenkäs, A., Sierra, C., Silva, V., Silva, M., Sitzia, T., Sjöman, H., Slot, M.,
705 Smith, N.G., Sodhi, D., Soltis, P., Soltis, D., Somers, B., Sonnier, G., Sørensen, M.V., Sosinski,
706 E.E., Soudzilovskaia, N.A., Souza, A.F., Spasojevic, M., Sperandii, M.G., Stan, A.B., Stegen, J.,
707 Steinbauer, K., Stephan, J.G., Sterck, F., Stojanovic, D.B., Strydom, T., Suarez, M.L.,
708 Svenning, J.C., Svitková, I., Svitok, M., Svoboda, M., Swaine, E., Swenson, N., Tabarelli, M.,
709 Takagi, K., Tappeiner, U., Tarifa, R., Tauugourdeau, S., Tavsanoglu, C., te Beest, M.,
710 Tedersoo, L., Thiffault, N., Thom, D., Thomas, E., Thompson, K., Thornton, P.E., Thuiller, W.,
711 Tichý, L., Tissue, D., Tjoelker, M.G., Tng, D.Y.P., Tobias, J., Török, P., Tarin, T., Torres-Ruiz,
712 J.M., Tóthmérész, B., Treurnicht, M., Trivellone, V., Trolliet, F., Trotsiuk, V., Tsakalos, J.L.,
713 Tsiripidis, I., Tysklind, N., Umehara, T., Usoltsev, V., Vadeboncoeur, M., Vaezi, J., Valladares,
714 F., Vamosi, J., van Bodegom, P.M., van Breugel, M., Van Cleemput, E., van de Weg, M., van
715 der Merwe, S., van der Plas, F., van der Sande, M.T., van Kleunen, M., Van Meerbeek, K.,
716 Vanderwel, M., Vanselow, K.A., Vårhammar, A., Varone, L., Vasquez Valderrama, M.Y.,
717 Vassilev, K., Vellend, M., Veneklaas, E.J., Verbeeck, H., Verheyen, K., Vibrans, A., Vieira, I.,
718 Villacís, J., Violle, C., Vivek, P., Wagner, K., Waldram, M., Waldron, A., Walker, A.P., Waller,

719 M., Walther, G., Wang, H., Wang, F., Wang, W., Watkins, H., Watkins, J., Weber, U.,
720 Weedon, J.T., Wei, L., Weigelt, P., Weiher, E., Wells, A.W., Wellstein, C., Wenk, E.,
721 Westoby, M., Westwood, A., White, P.J., Whitten, M., Williams, M., Winkler, D.E., Winter,
722 K., Womack, C., Wright, I.J., Wright, S.J., Wright, J., Pinho, B.X., Ximenes, F., Yamada, T.,
723 Yamaji, K., Yanai, R., Yankov, N., Yguel, B., Zanini, K.J., Zanne, A.E., Zelený, D., Zhao, Y.P.,
724 Zheng, Jingming, Zheng, Ji, Ziemińska, K., Zirbel, C.R., Zizka, G., Zo-Bi, I.C., Zotz, G., Wirth,
725 C., 2020. TRY plant trait database – enhanced coverage and open access. Glob. Chang. Biol.
726 26, 119–188. https://doi.org/10.1111/gcb.14904

727 Kennedy, D., Swenson, S., Oleson, K.W., Lawrence, D.M., Fisher, R., da Costa, A.C.L., Gentine, P.,
728 2019. Implementing plant hydraulics in the Community Land Model , version 5. J. Adv.
729 Model. Earth Syst. 11, 485–513. https://doi.org/10.1029/2018MS001500

730 Klesse, S., 2021. Critical note on the application of the “two-third” spline. Dendrochronologia 65,
731 125786. https://doi.org/10.1016/j.dendro.2020.125786

732 Kolus, H.R., Huntzinger, D.N., Schwalm, C.R., Fisher, J.B., Mckay, N., Fang, Y., Michalak, A.M.,
733 Schaefer, K., Wei, Y., Poulter, B., Mao, J., Parazoo, N.C., Shi, X., 2019. Land carbon models
734 underestimate the severity and duration of drought’s impact on plant productivity. Sci.
735 Rep. 9, 2758. https://doi.org/10.1038/s41598-019-39373-1

736 Körner, C., 2015. Paradigm shift in plant growth control. Curr. Opin. Plant Biol. 25, 107–114.
737 https://doi.org/10.1016/j.pbi.2015.05.003

738 Krejza, J., Haeni, M., Darenova, E., Foltýnová, L., Fajstavr, M., Světlík, J., Nezval, O., Bednář, P.,
739 Šigut, L., Horáček, P., Zweifel, R., 2022. Disentangling carbon uptake and allocation in the
740 stems of a spruce forest. Environ. Exp. Bot. 196, 104787.

741 https://doi.org/10.1016/j.envexpbot.2022.104787

742 Lloret, F., Keeling, E.G., Sala, A., 2011. Components of tree resilience: Effects of successive low-
743 growth episodes in old ponderosa pine forests. Oikos 120, 1909–1920.
744 https://doi.org/10.1111/j.1600-0706.2011.19372.x

745 Love, D.M., Venturas, M.D., Sperry, J.S., Brooks, P.D., Pettit, J.L., Wang, Y., Anderegg, W.R.L., Tai,
746 X., Mackay, D.S., 2019. Dependence of Aspen Stands on a Subsurface Water Subsidy:
747 Implications for Climate Change Impacts. Water Resour. Res. 55, 1833–1848.
748 https://doi.org/10.1029/2018WR023468

749 Maire, V., Wright, I.J., Prentice, I.C., Batjes, N.H., Bhaskar, R., van Bodegom, P.M., Cornwell,
750 W.K., Ellsworth, D., Niinemets, Ü., Ordonez, A., Reich, P.B., Santiago, L.S., 2015. Global
751 effects of soil and climate on leaf photosynthetic traits and rates. Glob. Ecol. Biogeogr. 24,
752 706–717. https://doi.org/10.1111/geb.12296

753 Martin-StPaul, N., Delzon, S., Cochard, H., 2017. Plant resistance to drought depends on timely
754 stomatal closure. Ecol. Lett. 20, 1437–1447. https://doi.org/10.1111/ele.12851

755 McDowell, N.G., Allen, C.D., Anderson-Teixeira, K., Aukema, B.H., Bond-Lamberty, B., Chini, L.,
756 Clark, J.S., Dietze, M., Grossiord, C., Hanbury-Brown, A., Hurtt, G.C., Jackson, R.B., Johnson,
757 D.J., Kueppers, L., Lichstein, J.W., Ogle, K., Poulter, B., Pugh, T.A.M., Seidl, R., Turner, M.G.,
758 Uriarte, M., Walker, A.P., Xu, C., 2020. Pervasive shifts in forest dynamics in a changing
759 world. Science (80-.). 368. https://doi.org/10.1126/science.aaz9463

760 Merlin, M., Perot, T., Perret, S., Korboulewsky, N., Vallet, P., 2015. Effects of stand composition
761 and tree size on resistance and resilience to drought in sessile oak and Scots pine. For. Ecol.

762 Manage. 339, 22–33. https://doi.org/10.1016/j.foreco.2014.11.032

763 Muhr, J., Messier, C., Delagrange, S., Trumbore, S., Xu, X., Hartmann, H., 2016. How fresh is
764 maple syrup? Sugar maple trees mobilize carbon stored several years previously during
765 early springtime sap-ascent. New Phytol. 209, 1410–1416.

766 Mund, M., Kutsch, W.L., Wirth, C., Kahl, T., Knohl, A., Skomarkova, M. V., Schulze, E.D., 2010.
767 The influence of climate and fructification on the inter-annual variability of stem growth
768 and net primary productivity in an old-growth, mixed beech forest. Tree Physiol. 30, 689–
769 704. https://doi.org/10.1093/treephys/tpq027

770 Pan, Y., Birdey, R.A., Fang, J., Houghton, R., Kauppi, P.E., Kurz, W.A., Phillips, O.L., Shcidenko, A.,
771 Lewis, S.L., Canadell, J.G., Ciais, P., Jackson, R.B., Pacala, S.W., McGuire, A.D., Piao, S.,
772 Rautianen, A., Sitch, S., Hayes, D., 2011. A large and persistent carbon sink in the world's
773 forests. Science (80-.). 333, 988–993. https://doi.org/10.1126/science.1201609

774 Pappas, C., Maillet, J., Rakowski, S., Baltzer, J.L., Barr, A.G., Black, T.A., Fatichi, S., Laroque, C.P.,
775 Matheny, A.M., Roy, A., Sonnentag, O., Zha, T., 2020. Aboveground tree growth is a minor
776 and decoupled fraction of boreal forest carbon input. Agric. For. Meteorol. 290, 108030.
777 https://doi.org/10.1016/j.agrformet.2020.108030

778 Pastorello, G., Trotta, C., Canfora, E., Chu, H., Christianson, D., Cheah, Y.W., Poindexter, C., Chen,
779 J., Elbashandy, A., Humphrey, M., Isaac, P., Polidori, D., Ribeca, A., van Ingen, C., Zhang, L.,
780 Amiro, B., Ammann, C., Arain, M.A., Ardö, J., Arkebauer, T., Arndt, S.K., Arriga, N., Aubinet,
781 M., Aurela, M., Baldocchi, D., Barr, A., Beamesderfer, E., Marchesini, L.B., Bergeron, O.,
782 Beringer, J., Bernhofer, C., Berveiller, D., Billesbach, D., Black, T.A., Blanken, P.D., Bohrer,
783 G., Boike, J., Bolstad, P. V., Bonal, D., Bonnefond, J.M., Bowling, D.R., Bracho, R., Brodeur,

J., Brümmer, C., Buchmann, N., Burban, B., Burns, S.P., Buysse, P., Cale, P., Cavagna, M., Cellier, P., Chen, S., Chini, I., Christensen, T.R., Cleverly, J., Collalti, A., Consalvo, C., Cook, B.D., Cook, D., Coursolle, C., Cremonese, E., Curtis, P.S., D'Andrea, E., da Rocha, H., Dai, X., Davis, K.J., De Cinti, B., de Grandcourt, A., De Ligne, A., De Oliveira, R.C., Delpierre, N., Desai, A.R., Di Bella, C.M., di Tommasi, P., Dolman, H., Domingo, F., Dong, G., Dore, S., Duce, P., Dufrêne, E., Dunn, A., Dušek, J., Eamus, D., Eichelmann, U., ElKhidir, H.A.M., Eugster, W., Ewenz, C.M., Ewers, B., Famulari, D., Fares, S., Feigenwinter, I., Feitz, A., Fensholt, R., Filippa, G., Fischer, M., Frank, J., Galvagno, M., Gharun, M., Gianelle, D., Gielen, B., Gioli, B., Gitelson, A., Goded, I., Goeckede, M., Goldstein, A.H., Gough, C.M., Goulden, M.L., Graf, A., Griebel, A., Gruening, C., Grünwald, T., Hammerle, A., Han, S., Han, X., Hansen, B.U., Hanson, C., Hatakka, J., He, Y., Hehn, M., Heinesch, B., Hinko-Najera, N., Hörtnagl, L., Hutley, L., Ibrom, A., Ikawa, H., Jackowicz-Korczynski, M., Janouš, D., Jans, W., Jassal, R., Jiang, S., Kato, T., Khomik, M., Klatt, J., Knohl, A., Knox, S., Kobayashi, H., Koerber, G., Kolle, O., Kosugi, Y., Kotani, A., Kowalski, A., Kruijt, B., Kurbatova, J., Kutsch, W.L., Kwon, H., Launiainen, S., Laurila, T., Law, B., Leuning, R., Li, Yingnian, Liddell, M., Limousin, J.M., Lion, M., Liska, A.J., Lohila, A., López-Ballesteros, A., López-Blanco, E., Loubet, B., Loustau, D., Lucas-Moffat, A., Lüers, J., Ma, S., Macfarlane, C., Magliulo, V., Maier, R., Mammarella, I., Manca, G., Marcolla, B., Margolis, H.A., Marras, S., Massman, W., Mastepanov, M., Matamala, R., Matthes, J.H., Mazzenga, F., McCaughey, H., McHugh, I., McMillan, A.M.S., Merbold, L., Meyer, W., Meyers, T., Miller, S.D., Minerbi, S., Moderow, U., Monson, R.K., Montagnani, L., Moore, C.E., Moors, E., Moreaux, V., Moureaux, C., Munger, J.W., Nakai, T., Neirynck, J., Nesic, Z., Nicolini, G., Noormets, A., Northwood, M., Nosetto, M., Nouvellon, Y., Novick, K., Oechel, W., Olesen, J.E., Ourcival, J.M., Papuga, S.A., Parmentier,

F.J., Paul-Limoges, E., Pavelka, M., Peichl, M., Pendall, E., Phillips, R.P., Pilegaard, K., Pirk, N., Posse, G., Powell, T., Prasse, H., Prober, S.M., Rambal, S., Rannik, Ü., Raz-Yaseef, N., Reed, D., de Dios, V.R., Restrepo-Coupe, N., Reverter, B.R., Roland, M., Sabbatini, S., Sachs, T., Saleska, S.R., Sánchez-Cañete, E.P., Sanchez-Mejia, Z.M., Schmid, H.P., Schmidt, M., Schneider, K., Schrader, F., Schroder, I., Scott, R.L., Sedlák, P., Serrano-Ortíz, P., Shao, C., Shi, P., Shironya, I., Siebicke, L., Šigut, L., Silberstein, R., Sirca, C., Spano, D., Steinbrecher, R., Stevens, R.M., Sturtevant, C., Suyker, A., Tagesson, T., Takanashi, S., Tang, Y., Tapper, N., Thom, J., Tiedemann, F., Tomassucci, M., Tuovinen, J.P., Urbanski, S., Valentini, R., van der Molen, M., van Gorsel, E., van Huissteden, K., Varlagin, A., Verfaillie, J., Vesala, T., Vincke, C., Vitale, D., Vygodskaya, N., Walker, J.P., Walter-Shea, E., Wang, H., Weber, R., Westermann, S., Wille, C., Wofsy, S., Wohlfahrt, G., Wolf, S., Woodgate, W., Li, Yuelin, Zampedri, R., Zhang, J., Zhou, G., Zona, D., Agarwal, D., Biraud, S., Torn, M., Papale, D., 2020. The FLUXNET2015 dataset and the ONEFlux processing pipeline for eddy covariance data. Sci. Data 7, 225. https://doi.org/10.1038/s41597-020-0534-3

Peters, R.L., Steppe, K., Cuny, H.E., De Pauw, D.J.W., Frank, D.C., Schaub, M., Rathgeber, C.B.K., Cabon, A., Fonti, P., 2021. Turgor – a limiting factor for radial growth in mature conifers along an elevational gradient. New Phytol. 229, 213–229. https://doi.org/10.1111/nph.16872

Phillips, R.P., Ibáñez, I., D'Orangeville, L., Hanson, P.J., Ryan, M.G., McDowell, N.G., 2016. A belowground perspective on the drought sensitivity of forests: Towards improved understanding and simulation. For. Ecol. Manage. 380, 309–320. https://doi.org/10.1016/j.foreco.2016.08.043

829 Pugh, T.A.M., Rademacher, T., Shafer, S.L., Steinkamp, J., Barichivich, J., 2020. Understanding
830 the uncertainty in global forest carbon turnover. Biogeosciences 17, 3961–3989.

831 Reichstein, M., Falge, E., Baldocchi, D., Papale, D., Aubinet, M., Berbigier, P., Bernhofer, C.,
832 Buchmann, N., Gilmanov, T., Granier, A., Grunwald, T., Havrankova, K., Ilvesniemi, H.,
833 Janous, D., Knohl, A., Laurila, T., Lohila, A., Loustau, D., Matteucci, G., Meyers, T., Miglietta,
834 F., Ourcival, J.M., Pumpanen, J., Rambal, S., Rotenberg, E., Sanz, M., Tenhunen, J., Seufert,
835 G., Vaccari, F., Vesala, T., Yakir, D., Valentini, R., 2005. On the separation of net ecosystem
836 exchange into assimilation and ecosystem respiration: Review and improved algorithm.
837 Glob. Chang. Biol. 11, 1424–1439. https://doi.org/10.1111/j.1365-2486.2005.001002.x

838 Rocha, A. V., Goulden, M.L., Dunn, A.L., Wofsy, S.C., 2006. On linking interannual tree ring
839 variability with observations of whole-forest CO2 flux. Glob. Chang. Biol. 12, 1378–1389.
840 https://doi.org/10.1111/j.1365-2486.2006.01179.x

841 Rollinson, C.R., Alexander, M.R., Dye, A.W., Moore, D.J.P., Pederson, N., Trouet, V., 2021.
842 Climate sensitivity of understory trees differs from overstory trees in temperate mesic
843 forests. Ecology 102, e03264. https://doi.org/10.1002/ecy.3264

844 Saatchi, S., Asefi-Najafabady, S., Malhi, Y., Aragão, L.E.O.C., Anderson, L.O., Myneni, R.B.,
845 Nemani, R., 2013. Persistent effects of a severe drought on Amazonian forest canopy. Proc.
846 Natl. Acad. Sci. U. S. A. 110, 565–570. https://doi.org/10.1073/pnas.1204651110

847 Schwalm, C.R., Anderegg, W.R.L., Michalak, A.M., Fisher, J.B., Biondi, F., Koch, G., Litvak, M.,
848 Ogle, K., Shaw, J.D., Wolf, A., Huntzinger, D.N., Schaefer, K., Cook, R., Wei, Y., Fang, Y.,
849 Hayes, D., Huang, M., Jain, A., Tian, H., 2017. Global patterns of drought recovery. Nature
850 548, 202–205. https://doi.org/10.1038/nature23021

851 Seftigen, K., Frank, D.C., Björklund, J., Babst, F., Poulter, B., 2018. The climatic drivers of
852 normalized difference vegetation index and tree-ring-based estimates of forest
853 productivity are spatially coherent but temporally decoupled in Northern Hemispheric
854 forests. Glob. Ecol. Biogeogr. 27, 1352–1365. https://doi.org/10.1111/geb.12802

855 Shen, W., Jenerette, G.D., Hui, D., Scott, R.L., 2016. Precipitation legacy effects on dryland
856 ecosystem carbon fluxes: Direction, magnitude and biogeochemical carryovers.
857 Biogeosciences 13, 425–439. https://doi.org/10.5194/bg-13-425-2016

858 Sierra, C.A., Müller, M., Metzler, H., Manzoni, S., Trumbore, S.E., 2017. The muddle of ages,
859 turnover, transit, and residence times in the carbon cycle. Glob. Chang. Biol. 23, 1763–
860 1773. https://doi.org/10.1111/gcb.13556

861 Sippel, S., Reichstein, M., Ma, X., Mahecha, M.D., Lange, H., Flach, M., Frank, D., 2018. Drought,
862 Heat, and the Carbon Cycle: a Review. Curr. Clim. Chang. Reports.
863 https://doi.org/10.1007/s40641-018-0103-4

864 Spawn, S.A., Sullivan, C.C., Lark, T.J., Gibbs, H.K., 2020. Harmonized global maps of above and
865 belowground biomass carbon density in the year 2010. Sci. Data 7, 1–22.
866 https://doi.org/10.1038/s41597-020-0444-4

867 Speer, J., 2012. Fundamentals of tree-ring research. The University of Arizona Press, Tucson, AZ.
868 https://doi.org/10.1002/gea.20357

869 Stocker, B.D., Zscheischler, J., Keenan, T.F., Prentice, I.C., Seneviratne, S.I., Peñuelas, J., 2019.
870 Drought impacts on terrestrial primary production underestimated by satellite monitoring.
871 Nat. Geosci. 12, 264–270. https://doi.org/10.1038/s41561-019-0318-6

872 Stokes, M.A., Smiley, T.L., 1999. An introduction to tree-ring dating. University of Arizona Press:
873 Tucson, AZ.

874 Team, R.C., 2021. R: A language and environment for statistical computing.

875 Teets, A., Fraver, S., Hollinger, D.Y., Weiskittel, A.R., Seymour, R.S., Richardson, A.D., 2017.
876 Linking annual tree growth with eddy-flux measures of net ecosystem productivity across
877 twenty years of observation in a mixed conifer forest. Agric. For. Meteorol. 249, 479–487.
878 https://doi.org/10.1016/j.agrformet.2017.08.007

879 Tuck, S.L., Phillips, H.R.P., Hintzen, R.E., Scharlemann, J.P.W., Purvis, A., Hudson, L.N., 2014.
880 MODISTools - downloading and processing MODIS remotely sensed data in R. Ecol. Evol. 4,
881 4658–4668. https://doi.org/10.1002/ece3.1273

882 Venturas, M.D., Sperry, J.S., Hacke, U.G., 2017. Plant xylem hydraulics: What we understand,
883 current research, and future challenges. J. Integr. Plant Biol. 59, 356–389.
884 https://doi.org/10.1111/jipb.12534

885 Vicente-Serrano, S.M., Beguería, S., López-Moreno, J.I., 2010. A multiscalar drought index
886 sensitive to global warming: The standardized precipitation evapotranspiration index. J.
887 Clim. 23, 1696–1718. https://doi.org/10.1175/2009JCLI2909.1

888 Vitasse, Y., Bottero, A., Cailleret, M., Bigler, C., Fonti, P., Gessler, A., Lévesque, M., Rohner, B.,
889 Weber, P., Rigling, A., Wohlgemuth, T., 2019. Contrasting resistance and resilience to
890 extreme drought and late spring frost in five major European tree species. Glob. Chang.
891 Biol. 25, 3781–3792. https://doi.org/10.1111/gcb.14803

892 Wenk, E.H., Falster, D.S., 2015. Quantifying and understanding reproductive allocation schedules

in plants. Ecol. Evol. 5, 5521–5538. https://doi.org/10.1002/ece3.1802

Wright, I.J., Reich, P.B., Westoby, M., Ackerly, D.D., Baruch, Z., Bongers, F., Cavender-Bares, J., Chapin, T., Cornelissen, J.H.C., Diemer, M., Flexas, J., Garnier, E., Groom, P.K., Gulias, J., Hikosaka, K., Lamont, B.B., Lee, T., Lee, W., Lusk, C., Midgley, J.J., Navas, M.-L., Niinemets, U., Oleksyn, J., Osada, N., Poorter, H., Poot, P., Prior, L., Pyankov, V.I., Roumet, C., Thomas, S.C., Tjoelker, M.G., Veneklaas, E.J., Villar, R., 2004. The worldwide leaf economics spectrum. Nature 428, 821–827. https://doi.org/10.1038/nature02403

Wu, X., Liu, H., Ciais, P., Flurin, B., Guo, W., Zhang, C., Magliulo, V., Pavelka, M., Liu, S., Huang, Y., Wang, P., Chi, C., Ma, Y., 2018. Differentiating drought legacy effects on vegetation growth over the temperate Northern hemisphere. Glob. Chang. Biol. 24, 504–516. https://doi.org/10.1111/gcb.13920

Wutzler, T., Lucas-Moffat, A., Migliavacca, M., Knauer, J., Sickel, K., Šigut, L., Menzer, O., Reichstein, M., 2018. Basic and extensible post-processing of eddy covariance flux data with REddyProc. Biogeosciences 15, 5015–5030. https://doi.org/10.5194/bg-15-5015-2018

Xu, K., Wang, X., Liang, P., An, H., Sun, H., Han, W., Li, Q., 2017. Tree-ring widths are good proxies of annual variation in forest productivity in temperate forests. Sci. Rep. 7. https://doi.org/10.1038/s41598-017-02022-6

Yang, Y., Saatchi, S.S., Xu, L., Yu, Y., Choi, S., Phillips, N., Kennedy, R., Keller, M., Knyazikhin, Y., Myneni, R.B., 2018. Post-drought decline of the Amazon carbon sink. Nat. Commun. 9. https://doi.org/10.1038/s41467-018-05668-6

Yu, K., Smith, W.K., Trugman, A.T., Condit, R., Hubbell, S.P., Sardans, J., Peng, C., Zhu, K.,

914 Peñuelas, J., Cailleret, M., Levanic, T., Gessler, A., Schaub, M., Ferretti, M., Anderegg,
915 W.R.L., 2019. Pervasive decreases in living vegetation carbon turnover time across forest
916 climate zones. Proc. Natl. Acad. Sci. U. S. A. 116, 24662–24667.
917 https://doi.org/10.1073/pnas.1821387116

918 Yu, Z., Wang, J., Liu, S., Rentch, J.S., Sun, P., Lu, C., 2017. Global gross primary productivity and
919 water use efficiency changes under drought stress. Environ. Res. Lett. 12, 014016.
920 https://doi.org/10.1088/1748-9326/aa5258

921
922
923
924
925
926
927
928
929
930

Figures

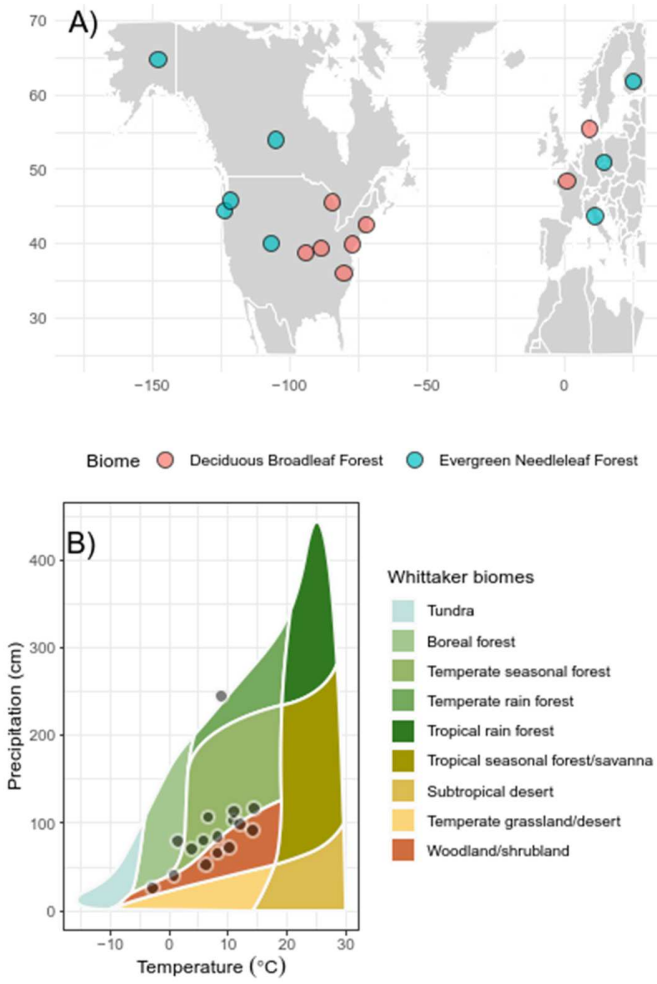

Figure 1. Map of all eddy covariance towers where tree-ring chronologies were collected (panel A), along with the climate space and biome that our sites represented (panel B).

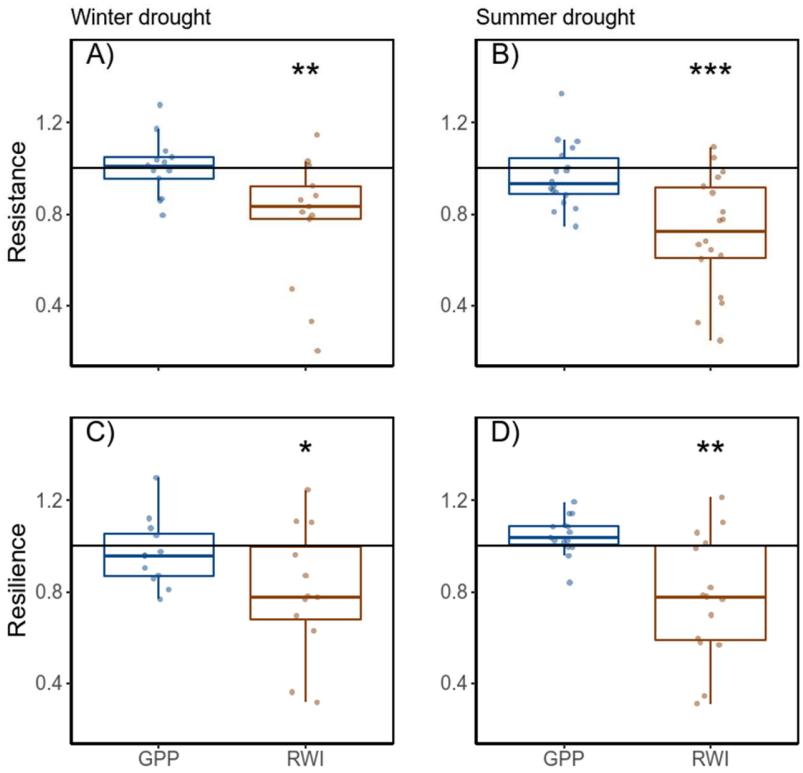

936

937 Figure 2. Resistance (Rt, panels A and B) and resilience (Rs, panels C and D) in normalized gross
938 primary productivity (GPP) and weighted tree-ring width (RWI) in response to two drought
939 periods: winter (October – March, panels A and C) and summer (June – August, panels B and D).
940 The horizontal line represents a value of one, which represents no response to drought. The *
941 symbol indicates a p-value < 0.05 for a t-test from one, ** indicates a p-value < 0.01, and ***
942 indicates a p-value < 0.001.

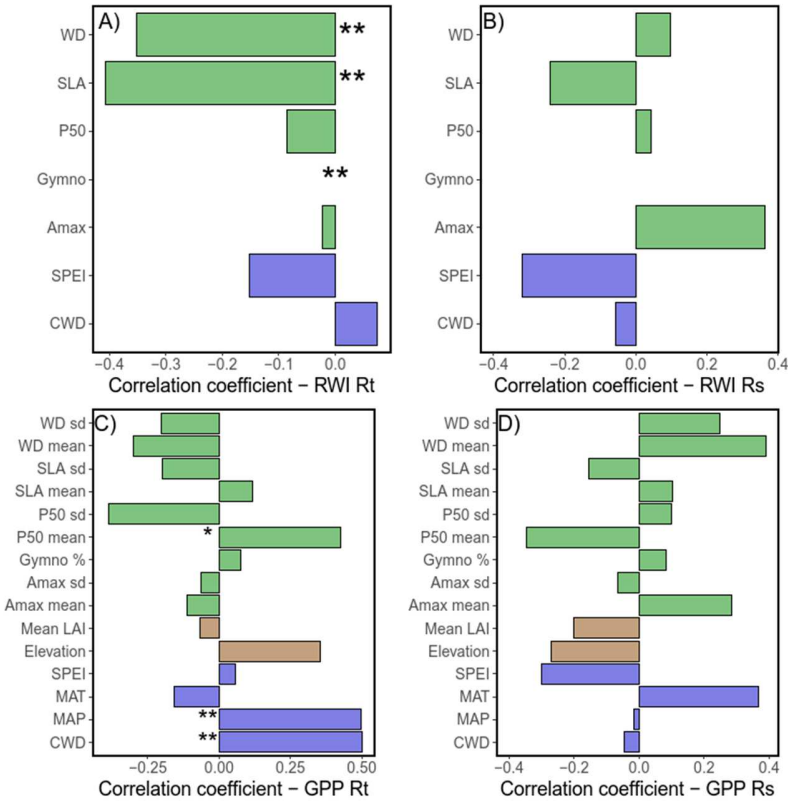

Figure 3. Pearson's correlation coefficients between Rt (panels A and C) and Rs (panel B and D) in weighted ring width (RWI, panels A and B) and normalized gross primary productivity (GPP, panels C and D) in response to summer droughts for all plant- and site-level traits, including maximum photosynthetic capacity (Amax), mean site climate water deficit (CWD), elevation, taxa (gymnosperm/angiosperm, or % gymnosperm species presence), mean annual temperature/precipitation (MAT/MAP), mean site leaf area index (Mean LAI), the water potential at 50% loss of conductivity (P50), specific leaf area (SLA), SPEI during the drought (SPEI), and wood density (WD). Bar color represents the type of trait: plant (green), climate (blue), or site (brown). The * symbol indicates a p-value < 0.1, while ** indicates a p-value < 0.05. Correlation coefficients are not present for the 'Gymno' trait as these relationships were assessed with t-tests.

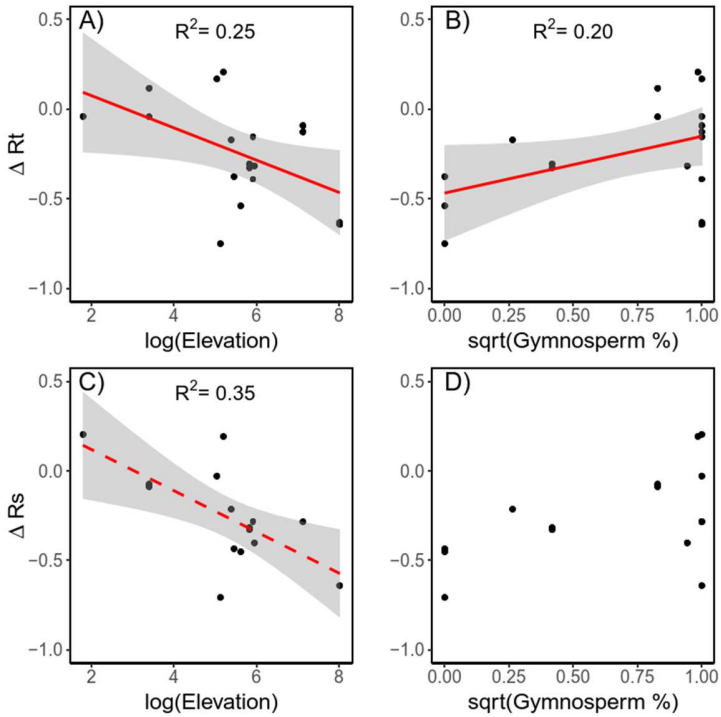

955

956 Figure 4. Relationships between tree-and site-level traits and ΔRt (panels A and B) or ΔRs (panels

957 C and D) in response to summer drought. Solid trendlines are present for significant

958 relationships ($p < 0.05$) and dotted lines represent moderately significant relationships ($p < 0.1$).

959

960

961

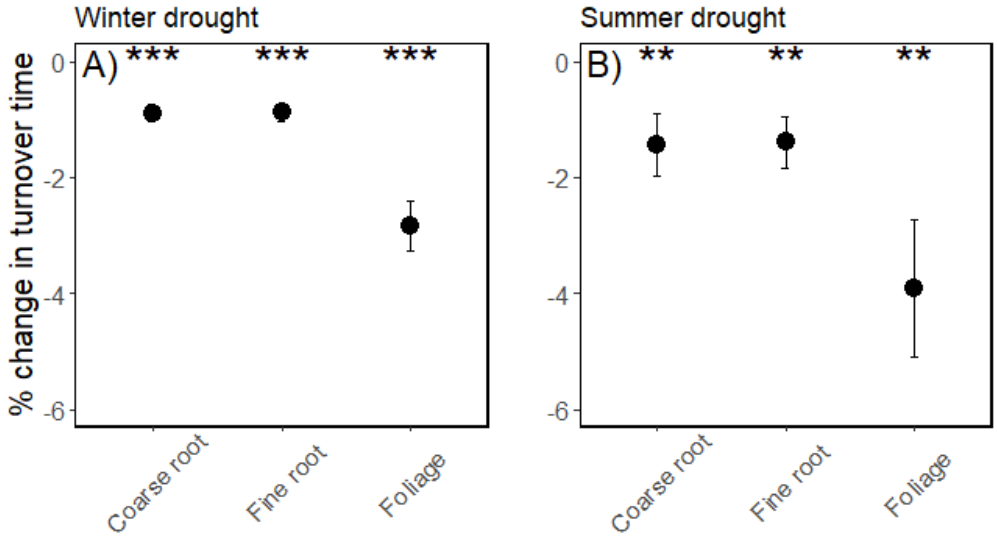

962

963 Figure 5. Change in whole-forest C turnover time in response to winter (panel A) and summer
964 (panel B) droughts based on simulations where the losses of tree ring C during, and following,
965 drought (i.e., Rt and Rs), are allocated entirely to coarse roots, fine roots, or leaves. Dots
966 represent the tissue mean and error bars represent standard error. The * symbol indicates a p-
967 value < 0.05 for a t-test from 0, ** indicates a p-value < 0.01, and *** indicates a p-value <
968 0.001.